

**Influence of the Atlantic Multidecadal Oscillation on  
the winter climate of East China**

Shuanglin Li and Gary T. Bates

(NOAA ESRL-CIRES Climate Diagnostics Center, University of Colorado, Boulder, Colorado)

Revised for AAS

June 2006

(submitted in August 2005)

Corresponding author:

Shuanglin Li, NOAA ESRL-CIRES CDC, R1/PSD, 325 Broadway, Boulder, CO 80305-3328

E-mail: [shuanglin.li@noaa.gov](mailto:shuanglin.li@noaa.gov)

## **Abstract**

The Atlantic Multidecadal Oscillation (AMO), the multidecadal variation of North Atlantic sea surface temperature (SST), exhibits an oscillation with period of 65-80 years and amplitude of 0.4°C. Observational composite analyses reveal that the warm-phase AMO is linked to warmer winters in East China with enhanced (reduced) precipitation in the northern (southern) China on multidecadal timescales. The pattern is reversed during the cold-phase AMO. Whether the AMO acts as a forcing on the multidecadal winter climate of East China is explored by investigating atmospheric response to warm AMO SST anomalies in a large ensemble of atmospheric general circulation model (AGCM) experiments. The results from three AGCMs are consistent and suggest that the AMO warmth favors warmer winters in East China. This influence is realized through inducing negative surface air pressure anomalies in the hemispheric-wide domain extending from the midlatitude North Atlantic to midlatitude Eurasia. These negative surface anomalies favor to weaken Mongolian Cold High, and thus induce a weaker East Asian Winter Monsoon.

## **1. Introduction**

Due to the short record of instrumental measurements and the presence of anthropogenic forcings such as the greenhouse gas concentration increase, it is challenging to understand the climate variability on multidecadal timescales. Global oceans are known to play important roles in climate system because of the big heat inertia and the slow movement of sea water. How sea surface temperatures (SSTs) vary on multidecadal timescales and how these variations influence climate have been being an important subject of climate research.

Both observational analyses (e.g., Schlesinger and Ramankutty, 1994) and naturally forced integrations of the coupled ocean-atmosphere model (Delworth and Mann, 2000) suggest a

multidecadal fluctuation pattern of North Atlantic SST variations. This pattern has a period of 65-80 years, and was referred to as the Atlantic Multidecadal Oscillation (AMO) by Kerr (2000). Its amplitude is  $0.4^{\circ}\text{C}$ , about half the standard deviation of annual mean SST. Figure 1a displays the historical evolution of an AMO index based on Enfield et al. (2001), while Fig. 1b depicts the SST difference between a warm-phase period (1935-55) and a cold-phase period (1970-90). This SST difference resembles the spatial pattern and has about twice the amplitude of the AMO (see Fig. 1b in Sutton and Hodson, 2005; also Fig. 1b in Enfield et al., 2001). The AMO is significant, since it can be isolated not only from annual mean data, but also from either summer or winter data (Sutton and Hodson, 2005). Its formation can be attributed to the fluctuations of northward heat transport associated with the Thermohaline Circulation (THC) (Delworth and Mann, 2000). Recent studies demonstrated that the AMO exerts significant influence on regional climate. For example, it is an important driver of multidecadal variations in the summertime climate of both North America and Europe, also a modulator of winter rainfall variability over the continental US (Sutton and Hodson, 2005; Enfield et al., 2001).

The AMO covers the entire North Atlantic Ocean basin. Various North Atlantic SST anomalies have been demonstrated previously to be able to influence East Asian winter climate on seasonal to interannual timescales. Lu's (2005) atmospheric general circulation model (AGCM) simulations on the annual climate for 1998 climate year, the warmest in the record of instrumental measurements, revealed that 1998's Pan-Atlantic SST have significantly contributed to the anomalous global land surface air temperature, and have played a substantial role in forming the anomalous East Asian winter monsoon of that year. The 1998 SST anomalies have a northern component obviously projecting on the AMO (cp. Fig. 1 in Lu (2005) with Fig. 1b here). Li's (2004) observational analyses and large-size ensemble AGCM simulations suggest that northwest

Atlantic Ocean warmth, which largely overlaps over the maximum center of the AMO (cp. Fig. 4 with Fig. 1b here), induces one wave-like 500-hPa height response chain extending from the North Atlantic to Eurasia with a positive response over the Ural Mountains in early winter, and subsequently results in less outbreaks of cold air in East Asia. Besides, the North Atlantic circulation anomaly, especially the North Atlantic Oscillation (Arctic Oscillation) (NAO/AO), the most significant circulation variability in the northern hemisphere on various timescales, was revealed to be associated with anomalous East Asian Winter Monsoon (EAWM) on the interannual or interdecadal timescales. Gong et al.'s (2001) observational analyses indicated that significant positive correlations of the AO Index exist with the winter surface temperature in East China on the interannual timescales. Thompson and Wallace (2001) found a similar association. In contrast, more recently, Wu et al. (2006) found that the NAO/AO influence on EAWM is primarily on the interdecadal time scales, and, furthermore, the EAWM is independent on the NAO/AO on the interannual time scales. No matter on whatever time scales, the NAO, albeit primarily arisen from the atmospheric internal variability, can be forced by a North Atlantic SST tripolar pattern (Sutton et al., 2000; Peng et al., 2003; Li et al., 2006). Thus, this SST tripolar pattern should influence EAWM on the interannual or interdecadal time scales. Since these various North Atlantic SSTAs may influence EAWM on various time scales, whether and how the AMO exerts significant influence on the winter climate of East Asia, especially East China, on the multidecadal time scales are intriguing but unclear. This motivates the present study.

As mentioned above, it is difficult to perform a comprehensive empirical analysis on the link between the AMO and the multidecadal East China winter variability due to an insufficiently long climate series (Wang et al., 2004). Nonetheless, a comparison between the composites when the AMO is positive and negative may give indications. A simple observational composite is thus

performed for two AMO extreme phase periods, a warm period from 1935 to 1955 and a cold period from 1970-1990 (see Fig. 1a), within the 20<sup>th</sup> century when relatively reliable observed data is available. Since observational association is not casual, AGCMs are employed to investigate the climate influence of the AMO warmth. Rather than isolate AMO contribution rate from the model responses with blended miscellaneous forcings, we investigate direct atmospheric response to an isolated warm-phase AMO SSTA by conducting AMIP (Atmospheric Model Inter-comparison Project) experiments. In view of the model response sensitivity to the experiment sampling, large-ensemble experiment is used. To verify possible dependence of the response on the model used, three AGCMs are used in this study.

This paper is organized as follows. Observational composite analyses are performed in section 2. Section 3 describes the models and experiment design. The modeled climate responses and the associated large-scale circulation are analyzed in section 4. A brief summary and discussions are given in the last section.

## **2. Observational analyses**

Global monthly surface air temperature (Ts) anomaly, gridded at 5.0 latitude by 5.0 longitude, from 1873-1999 (Jones and Moberg, 2003), northern hemispheric monthly sea level pressure (SLP), gridded at 5.0 latitude spanning 15°N to 85°N by 10.0 longitude, from 1873-1999 (Basnett and Parker, 1997), and global land-area monthly precipitation (Precip), gridded at 2.5 latitude by 3.75 longitude, through 1900-1999 (Hulme, 1992) from the Climate Research Unit (CRU), British Meteorological Office are used. These datasets are referred to as CRU's Ts and SLP, and Hulme's Precip, respectively. Neither all grids nor all times throughout their whole data periods have values uniformly in these datasets. Because of a significant linear warming trend since

the middle 19<sup>th</sup> century, all these datasets are detrended first. One check calculation suggests that this processing has significant influence on Ts, but little on SLP and Precip, consistent with Wang et al. (2004). Since the multidecadal variability is concerned, a 10-year running mean is then applied to the detrended series.

These CRU datasets are not derived uniformly from the instrumental measurement. One more reliable dataset, the observed monthly surface air temperature and precipitation in 160-stations of mainland China since 1951 are used as a supplement<sup>1</sup>. It is referred to as China 160-station dataset. Similarly, the linear trend is removed from it. Due to the short record length, no further filter is applied to it.

The composite when the AMO is warm (1935/36 to 1955/56) is found to be largely opposite to that when the AMO is cold (1970/71 to 1990/91). For brevity the composite difference between these two extreme phase periods is analyzed here. Such difference represents doubled anomaly associated with the AMO. Figure 2 displays the results of the November-February (NDJF) mean Hulme's precipitation anomaly percentage, CRU's Ts, and SLP. No Hulme's precipitation data is available in west China, so the sector is blanked in Fig. 2a. In general, East China is warmer and wetter, except the southern coastal area. The mean warming (cooling) is 0.2-0.3°C when the AMO is positive (negative). It seems reasonable that a warmer winter has more precipitation, since there is more vapor evaporation from warmer surface, and thus tends to induce more precipitation.

The observed circulation anomaly associated with the AMO is further analyzed. Along with East China warmer winters, there are negative SLP anomalies extending from northeastern North Atlantic to midlatitudal East Asia and positive anomalies in the northern high-latitudinal and polar area (Fig. 2c). This SLP pattern is reminiscent of the negative-phase AO, albeit its maximum

---

<sup>1</sup> The China 160-station precipitation and temperature dataset was provided by the National Climate Center of China Meteorological Administration.

positive is shifted to Siberia. In particular, SLP anomalies over Mongolia are negative, weakening Mongolian Cold High. This correspondence between warmer East China winters and weakened Mongolian Cold High is in agreement with the negative correlation between Siberia high and East China winter surface air temperature on interannual timescales (Gong et al., 2001).

The observed SLP association with the AMO was reflected in part in previous studies. Kushnir (1994) analyzed time series of SST spanning the period 1900-1987 over the North Atlantic, and obtained AMO-like multidecadal SST fluctuations. The spatial patterns of the SLP associated with the positive SSTA have an anomalous low pressure over the central North Atlantic at about 45°N and an anomalous high poleward of 60°N, largely in agreement with the present analysis. Sutton and Hodson (2003) separated the multidecadal air-sea variability from the interannual variability, and demonstrated that the SLP pattern associated with the multidecadal North Atlantic SST variation (AMO, albeit they did not name it) also exhibits substantial negative anomalies over the central North Atlantic extending to Eurasia (see their Figs. 5b and c). One modest discrepancy between the present SLP composite and the previous is the shift of the maximum negative anomaly over the central North Atlantic to southern Europe. This may be attributed to a different SLP dataset.

The above association between the East China winter climate and the AMO is seen more clearly in the composites based on China 160-station dataset (Fig. 3), albeit a shorter period is used to construct the composite for the AMO warm phase. When the AMO is warm phase, East China winter is warmer than normal, and also wetter except the southern coastal area. It is contrary when the AMO is cold phase. This consistency between these different datasets suggests the observed multidecadal wintertime climate variation in East China may be strongly related to the AMO.

### 3. AGCMs and experiment design

Whether the AMO acts as one forcing on winter climate of East China is addressed by investigating atmospheric response to the AMO SST anomaly through AGCM sensitive experiments. Three AGCMs are used here. The first is the National Centers for Atmospheric Research (NCAR)'s Community Climate Model Version 3.0 (CCM3, Kiehl et al., 1998). Two sets of ensembles with 40-members, starting from different initial fields and integrating for 13 months from September to next September, are performed. These 40 initial fields are from restart files of previous experiments. Ensemble one, referred to as the control ensemble, is formed from the runs forced with climatological SST seasonal cycle. Ensemble two, referred to as the SSTA ensemble, is from the runs with the SSTA in Fig.1b added on the climatological SST seasonal cycle. Thus, total 40 model years are available for analysis in each ensemble.

The second AGCM is one earlier version of NCEP (National Centers for Environment Prediction) AGCM for seasonal prediction, and one updated version was described by Kanamitsu (2001). Similar to the CCM3, two sets of ensembles but with 60-members each are performed. The 60 initial fields are from the NCEP-NCAR reanalysis of 00UTC, 1-3 September 1980-1999 (Kalnay et al., 1996). Thus, total 60 model years are available for analysis in each ensemble.

The last AGCM is the GFDL (Geophysical Fluid Dynamics Laboratory)'s Atmospheric Model (AM2) (the GFDL Global Atmospheric Model Development Team, 2004). Two sets of ensemble 25 year integrations were performed: the first, the control ensemble, is forced with the climatological seasonally-evolving SST, and the second, the SSTA ensemble, is forced with the SSTA in Fig. 1b added on the climatological SST cycle. Initial field were obtained from the GFDL public release version. The first model year of each simulation is discarded to allow for model spin-up. Thus, there are total 48 model years for analysis in each ensemble.

All above experiments are summarized into Table 1. The November-February mean difference in the SSTA ensembles minus the control ensembles yields the atmospheric response. A Student's t-test is used to determine the significance of the response. Noteworthily, the SSTA in Fig. 1b is the difference of an AMO warm period minus a cold period. It represents double-enhanced AMO SSTA. It is meaningful to compare the model response to this SSTA to the composite difference of the AMO warm period minus the cold period under a linear scenario.

## 4. Modeling results

### 4.1 Regional climate response

Figure 4 shows precipitation anomaly percentage and Ts response. The precipitation response (left panels) in these three AGCMs is less significant, albeit one signal that northern East China is wetter while the southern coastal area is drier is discernable. However, the modeled less-precipitation area in the southern coast of East China extends farther to the north than the observational composite. In comparison, there are significantly warmer Ts responses in East China, largely consistent among these three AGCMs (right panels). These Ts responses bear some resemblance to the observed composites (cp. Fig. 4 with Figs. 2 and 3), and their maximum values are within 0.3-0.8°C. As mentioned previously, the SSTA used represents the doubled AMO anomalies, thus the model AMO influence should be scaled from the present simulated responses by the factor, 2. This yields the 0.2-0.4°C Ts response value, largely close to the value of 0.2-0.3°C based on the observational composite analysis. Thus, East China in winter is 0.2-0.3°C warmer (colder) than the normal during the AMO warm (cold).

Comparing the modeled response in these three AGCMs, one can see no significant Ts response over the northern sector from Siberia to Northeast China in the GFDL AM2 (Fig. 4f),

which is different from the two other AGCMs. This difference is associated with a modest shift of the modeled large-scale circulation response, which will be discussed in the next sub-section.

In comparison to Sutton and Hodson (2006), who performed similar experiments using one version of the UK Hadley Center AGCM, HadAM3, Ts bears considerable resemblance to their December-February response (see their Fig. 3c). There are significant warm Ts responses over Europe and East Asia including East China. This suggests that the AMO warmth induces warmer East China winters is independent on the model used. Similarly, the precipitation response in Sutton and Hodson (2006) is less significant (see their Fig. 3b).

#### *4.2 Large-scale circulation response*

As noted in Li et al. (2003), any modeled influence of the SST is of interest only if it arises from physically reasonable and realistic interactions within large-scale atmospheric circulation. Figure 5 displays 1000-hPa and 500-hPa geopotential height responses. The 1000-hPa height is used to represent surface pressure response, since not all these three AGCMs have SLP output. From Figs. 5b, d, and f, 1000-hPa responses are largely consistent in these models, especially over the hemispheric-wide sector from the North Atlantic extending eastward to Eurasia. There are strong negative surface responses over the northeastern Atlantic consistently in all these three AGCMs, although the locations of their maximum are not exactly coincident. There are also significant negative responses over northern Eurasia, with the maximum over west Siberia for both the CCM3 and NCEP AGCM. In comparison, the Asian negative SLP response in the AM2 is weaker, and has its maximum shift to Mongolia. Besides, there are positive surface responses over the northern polar area consistently in these AGCMs.

In comparison to previous model results, these 1000-hPa height responses are largely in agreement with the winter (DJF) SLP in Sutton and Hodson (2006) (see their Fig. 3a). For example, there are also substantially negative SLP responses throughout the North Atlantic to Eurasia, along with strong and positive SLP responses over the North Pacific (not shown). This indicates that the negative surface pressure response over this wide area is independent on the model.

The modeled 1000-hPa height responses, especially in both the NCEP AGCM and the AM2, bear some resemblance to the observational SLP composite (Fig. 2c), which appears more evident when the hemispheric-wide scale is concerned. There are zonally-extended negative 1000-hPa height responses along the mid-latitudes ( $\sim 55^{\circ}\text{N}$ ) largely circumcising the sign-reversed height response over the polar cap (Figs. 5d and f), and one similar pattern exists in Fig. 2c, albeit the negative SLP belt is more meridionally confined into southern latitudes. Visually, the biggest discrepancy is over northern Eurasia, with a strong positive SLP anomaly in the observational composite but not in the simulated responses. However, this observational strong positive SLP anomaly is less significant (see Fig. 7a in Sutton and Hodson, 2006).

The negative SLP response over southern Siberia and Mongolia is one common feature in these three AGCMs. It favors a weaker Siberia high, subsequently weaker East Asia winter monsoon and warmer Ts in East China (Gong et al. 2001). Thus, the consistently warm Ts response over East China in these AGCMs should be attributed to the anomalous circulation revealed in the 1000-hPa height responses. This suggests that the influence of the AMO SSTA on East China winters is realized through weakening Siberian/Mongolian High.

For the 500-hPa height response (Figs. 5a, c, e), there is a tripolar pattern over the North Atlantic in all these three AGCMs, with negative values over the midlatitude North Atlantic in-between positive values over Greenland and over subtropical North Atlantic. The subtropical

Atlantic positive response extends eastward to the northeastern Asia. Parallel to these across-continent positive responses, the midlatitudinal North Atlantic negative response extends to the east. When the surface responses are compared to these 500-hPa height responses, one correspondence is easily seen. For example, the primary negative surface responses are underlying negative 500-hPa height response. This further suggests that the modeled East Asia warming response to the AMO arises from the model's large-scale circulation interaction.

## **5. Summary and discussions**

Previous studies reveal that the AMO governs North American and European summer climates on the multidecadal time scales (Sutton and Hodson 2005; Enfield et al. 2001). The AMO SSTA covers the entire North Atlantic basin, and its formation has been attributed to the northward heat transport fluctuations associated with the Thermohaline Circulation (THC) (Delworth and Mann, 2000). Whether the AMO influences East China multidecadal winter climate is investigated. Both observational analyses and AGCM experiments are conducted. Rather than isolate the AMO influence from the experiments with blended various forcing, we investigate direct atmospheric response to an isolated warm-phase AMO SSTA by conducting AMIP runs. Three AGCMs, NCAR CCM3 and NCEP AGCM as well as GFDL AM2, are used. The results suggest that the AMO SSTA acts as a forcing on winter climate of East China. When the AMO is warm, East China winters tend to be warmer, and wetter in the wide northern area than normal. The warming strength is about 0.2-0.4°C for the typical AMO amplitude. This AMO influence is realized through inducing negative surface pressure anomalies over the hemispheric-wide domain across midlatitudinal North Atlantic extending eastward to midlatitudinal Eurasia. The surface air pressure anomalies over midlatitudinal Asian continent favor a weaker Mongolian Cold High, and thus a

weaker East Asian Winter monsoon. The large-scale circulation pattern associated with this climate response in both the models and the observations is largely consistent.

Significant winter climate variations in China on the multidecadal time scales were documented previously (e.g., Wang et al., 2004). The temporal variation of the detrended low-frequency annual mean temperature of East China bears an overall consistence in phase with the AMO index (cp. Fig.3 in Wang et al. with Fig. 1a). The AMO may have contributed to climate variation of East China in the 20<sup>th</sup> century along with the anthropogenic forcing.

Whether the present results have implications for the prediction of the next few decades is intriguing. From Fig.1a, the AMO is entering a warm phase period, and thus tends to induce warmer winters in East China. If this influence overlaps with the warming linear trend due to anthropogenic effect arisen from the increased greenhouse gas concentrations, East China will experience much warmer winters than before in the next decades. However, in reality, the climate variation in this domain may be much more complicated. Evidence suggests a negative feedback between the AMO and the global warming through the THC, since the global warming tends to slow down, even shut down, the THC because of both high-latitude warming and enhanced poleward atmospheric moisture transport (Houghton et al. 2001). Besides, the Pacific Decadal Oscillation (PDO), albeit with a shorter time scale than the AMO (Mantua et al., 1997), is known playing a role in modulating East China climate variations on interdecadal timescales (Li et al., 2004). The PDO can be influenced by the THC variations through atmospheric feedback (Dong and Sutton 2002). Aside from these oceanic effects, this winter climate multidecadal variation can be influenced by the other components of the climate system. For example, the sea ice concentration anomalies over the North Atlantic can act as a role (Alexander et al., 2004). Therefore, real climate variations in next decades depend on the interactions between the oceanic forcings including the

AMO, the THC and the PDO, also between the atmosphere and the other climate sub-systems, as well as the anthropogenic effect.

Since only the idealized AMO SST warmth is used to force the AGCMs in this study, one may wonder the existence of a similar atmospheric response to AMO signals in real historical-evolving SST. One four-member ensemble with the Météo-France ARPEGE AGCM prescribed with the historical North Atlantic SST through 1947-1998 in one recent study (Hoerling et al., 2006) indeed suggests this existence (no plots shown), albeit only part of AMO warm-phase period is covered in those experiments. Nevertheless, more comprehensive experiments with historical evolving SST and external forcing are needed in resolving this issue.

At last, the results from the observational analyses needs further verified because of the lack of a uniformly long instrumental records. Most of comparisons on the modeled responses with the observational composites are qualitative, not quantitative. The mechanism responsible for the modeled circulation anomaly needs further study.

**Acknowledgements.** The authors thank Dr. Martin P. Hoerling for helpful discussions, thank two anonymous reviewers for constructive critiques and suggestions that led to significant improvements in the manuscript, also thank Taiyi Xu for providing the ARPEGE experiment results for the comparison in the discussion section. This study was funded by NOAA's Office of Global Programs.

## REFERENCES

- Alexander, M. A., U. S. Bhatt, J. E. Walsh, M. S. Timlin, J. S. Miller and J. D. Scott, 2004: The atmospheric response to realistic Arctic sea ice anomalies in an AGCM during Winter. *J. Climate*, **17**, 890-905.
- Basnett, T.A. and Parker, D.E., 1997: Development of the Global Mean Sea Level Pressure Data Set GMSLP2. Climatic Research Technical Note No. 79. Hadley Centre, Meteorological Office, Bracknell, 16pp plus Appendices.
- Delworth, T. L., and M.E. Mann, 2000: Observed and simulated multidecadal variability in the Northern Hemisphere. *Clim. Dyn.*, **16**, 661-676.
- Dong, B.-W., and R. T. Sutton, 2002: Adjustment of the coupled ocean-atmosphere system to a sudden change in the Thermohaline Circulation, *Geophys. Res. Lett.*, **29**(15), 1728, 10.1029/2002GL015229.
- Enfield, D.B, A.M. Mestas-Nunez, and P.J. Trimble, 2001: The Atlantic multidecadal oscillation and its relation to rainfall and river flows in the continental U.S.. *Geophys. Res. Lett.*, **28**(10), 2077-2080.
- Gong Daoyi, Wang Shaowu, and Zhu Jinhong, 2001: East Asian winter monsoon and Arctic Oscillation. *Geophys. Res. Lett.*, **28**(10), 2073-2076.
- Hoerling, M. P., J. W. Hurrell, and J. Eischeid, 2006: Detection and attribution of twentieth-century northern and southern African rainfall change. *J. Climate*, in press.
- Houghton, J. T., Y. Doing, D. J. Griggs, M. Nigger, P. J. van der Linden, X. Pan, K. Maskell, and C. A. Johnson, 2001: *Climate Change 2001: The Scientific Basis*. Cambridge University Press, 881 pp.

- Hulme, M., 1992: 1951-80 global land precipitation climatology for the evaluation of general circulation models. *Clim. Dyn.*, **7**, 57-72.
- Jones, P.D. and Moberg, A., 2003: Hemispheric and large-scale surface air temperature variations: An extensive revision and an update to 2001. *J. Climate*, **16**, 206-223.
- Kalnay, E., et al., 1996: The NCEP/NCAR 40-year reanalysis project. *Bull. Amer. Meteor. Soc.*, **77**, 437-471.
- Kanamitsu, M., and co-authors, NCEP dynamical seasonal forecast system 2000. *Bull. Amer. Meteor. Soc.*, **83**, 1019-1037, 2002.
- Kerr, R. A., 2000: A north Atlantic climate pacemaker for the centuries. *Science*, **288**(5473), 1984-1986.
- Kiehl, et al., 1998: The National Center for Atmospheric Research Community Climate Model: CCM3. *J. Climate*, **11**, 1131-1149.
- Kushnir, Y., 1994: Interdecadal variations in North Atlantic sea surface temperature and associated atmospheric conditions. *J. Climate*, **7**, 141-157.
- Li Chongying, He Jinhai, and Zhu Jinhong, 2004: A review of decadal/interdecadal climate variation studies in China. *Adv. Atmos. Sci.*, **21**(3), 425-436.
- Li Shuanglin, W. A. Robinson, and Peng Shiling, 2003: Influence of the North Atlantic SST tripole on northwest African rainfall. *J. Geophys. Res.*, **108**(D19), 4594, doi:10.1029/2002JD003130.
- Li Shuanglin, 2004: Impact of Northwest Atlantic SST anomalies on the circulation over the Ural Mountains during early winter. *J. Meteor. Soc. Japan*, **82**(4), 971-988.
- Li Shuanglin, M. P. Hoerling, and Peng Shiling, 2006: Coupled ocean-atmosphere response to Indian Ocean warmth. *Geophys. Res. Lett.*, **33**(7), L07713, 10.1029/2005GL025558.

- Lu Riyu, 2005: Impact of Atlantic sea surface temperatures on the warmest global surface air temperature of 1998. *J. Geophys. Res.*, **110**, D05103, doi:10.1029/2004JD005203.
- Mantua, N.J., S. R. Hare, Y. Zhang, J.M. Wallace, and R. C. Francis, 1997: A Pacific decadal climate oscillation with impacts on salmon production. *Bull. Amer. Meteor. Soc.*, **78**, 1069-1079.
- Peng Shiling, W. A. Robinson, and Li Shuanglin, 2003: Mechanisms for the NAO responses to the North Atlantic SST tripole. *J. Climate*. **16**(12), 1987-2004.
- Schlesinger, M.E., and N. Ramankutty, 1994: An oscillation in the global climate system of period 65-70 years. *Nature*, **367**, 723-726.
- Sutton, R. T., W. A. Norton, and S. P. Jewson, 2000: The North Atlantic Oscillation-what role for the ocean?. *Atmos. Sci. Lett.*, DOI 10.1006/asle.2000.0018.
- Sutton, R.T., and D.L.R. Hodson, 2003: Influence of the Ocean on North Atlantic climate variability 1981-1999. *J. Climate*, **16**, 3296-3313.
- Sutton, R.T., and D.L.R. Hodson, 2005: Atlantic Ocean forcing of North American and European summer climate. *Science*, **309**, 115-118.
- Sutton, R.T., and D.L.R. Hodson, 2006: Climate response to multidecadal warming and cooling of the North Atlantic Ocean. *J. Climate*, (submitted).
- The GFDL Global Atmospheric Model Development Team, 2004: The new GFDL global atmosphere and land model AM2/LM2: Evaluation with prescribed SST simulations. *J. Climate*, **17**(24), 4641-4673.
- Thompson, D.W.J., and J. M. Wallace, 2001: Regional climate impacts of the northern hemisphere annular mode. *Science*, **293**, 85-89.

Wang Shaowu, Zhu Jinhong, and Cai Jingning, 2004: Interdecadal variability of temperature and precipitation in China since 1880. *Adv. Atmos. Sci.*, **21**(4), 307-313.

Wu B., Zhang R., and R. D'Arrigo, 2006: Distinct modes of East Asian winter monsoon. *Mon. Wea. Rev.*, in press.

Table .1 Summary of Experiments

Model (integration period)	NCAR CCM3 (13 months)	NCEP AGCM (13 months)	GFDL AM2 (25 years)
Control run	40	60	2
AMO warmth	40	60	2

## Figure Captions

Figure 1. (a) Temporal evolution of the AMO Index reproduced on basis of Enfield et al. (2001).

(b) Difference of the annual mean SSTA through 1935-1955 (AMO warm phase period, denoted by the lower horizontal solid line in (a)) minus the mean through 1970-90 (AMO cold phase period, denoted by the upper line in (a)). Unit in (a, b): °C. The contour interval in (b) is 0.25, and the contour 0.1 is displayed additionally. Kaplan Extended SST dataset (version 2) through 1856-2004 is used, which was processed by Lomont-Doherty Earth Observatory and was downloaded online from the NOAA Climate Diagnostics Center website: [www.cdc.noaa.gov](http://www.cdc.noaa.gov). Both the index and the difference are calculated from detrended, 10-year running mean filtered monthly SSTA.

Figure 2. (a) Difference of composite precipitation anomaly percentage (unit: %) for the winters (NDJF) of the AMO warm period (1935/56 - 1955/56) minus the cold period (1970/71-1990/91). (b), as (a), but surface air temperature anomaly (unit: °C). (c), as (a), but sea level pressure (unit: hPa). Shading represents the precipitation anomaly percentage greater (less) than 5% (-5%) in (a),  $T_s$  greater than 0.2 in (b), and SLP greater (less) than 0.5 (-0.5) in (c). The contour “0” is omitted in (c). The climatological precipitation used to derive the precipitation anomaly percentage in (a) is the mean through 1951-1980.

Figure 3. (a) Composite precipitation anomaly percentage when the AMO is warm (1951/52 - 1955/56). (b), as (a), but when the AMO is cold (1970/71-1990/91). (c) (d), as (a) (b), but surface air temperature anomaly. China 160 station dataset is used. Positive (negative) precipitation anomaly percentage values are plotted in blue (red) in (a, b) to indicate being wetter (drier), while sign-reversed  $T_s$  values are plotted in these two colors in (c, d) to indicate being colder (warmer). Unit: % in (a, b), and 0.1°C in (c, d).

Figure 4. (a) November-February mean response of precipitation anomaly percentage (unit: %) in the NCAR CCM3. (b) (c), as (a), but in the NCEP AGCM and the GFDL AM2, respectively. (d, e, f), as (a, b, c), but for surface air temperature (unit: °C). Shading indicates significant at the level of 95%.

Figure 5. As Fig. 4, but the response of 500-hPa and 1000-hPa geopotential heights. Unit: m.

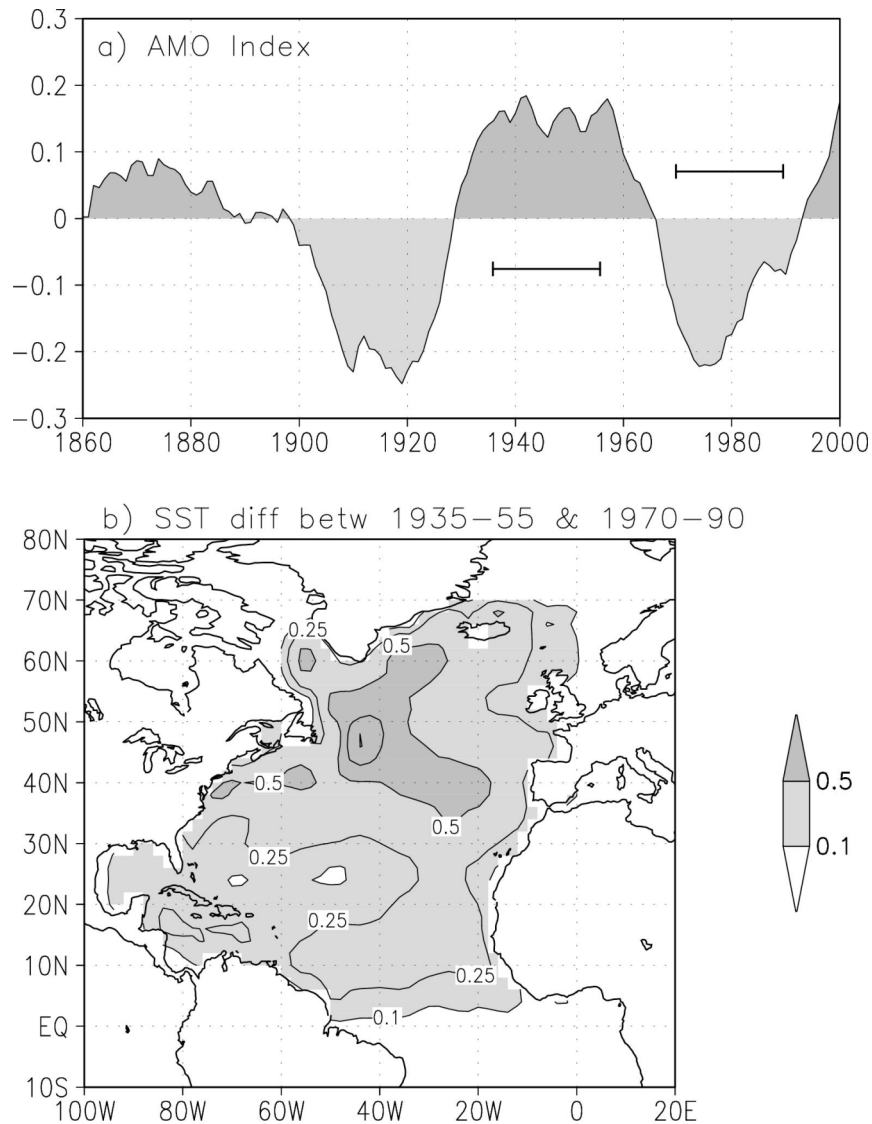


Figure 1. (a) Temporal evolution of the AMO Index reproduced from Enfield et al. (2001). (b) Difference of the annual mean SSTA through 1935-1955 (AMO warm phase period, denoted by the lower horizontal solid line in (a)) minus the mean through 1970-90 (AMO cold phase period, denoted by the upper horizontal solid line in (a)). Unit in (a, b):  $^{\circ}\text{C}$ . The contour interval in (b) is 0.25, and the contour 0.1 is also displayed. Kaplan Extended SST dataset (version 2) through 1856-2004 is used, which was processed by Lomont-Doherty Earth Observatory and was downloaded online from the NOAA Climate Diagnostics Center website: [www.cdc.noaa.gov](http://www.cdc.noaa.gov). Both the index and the difference are calculated from detrended, 10-year running mean filtered monthly SSTA.

Warm – Cold  
(1935/36–55/56) – (1970/71–90/91)

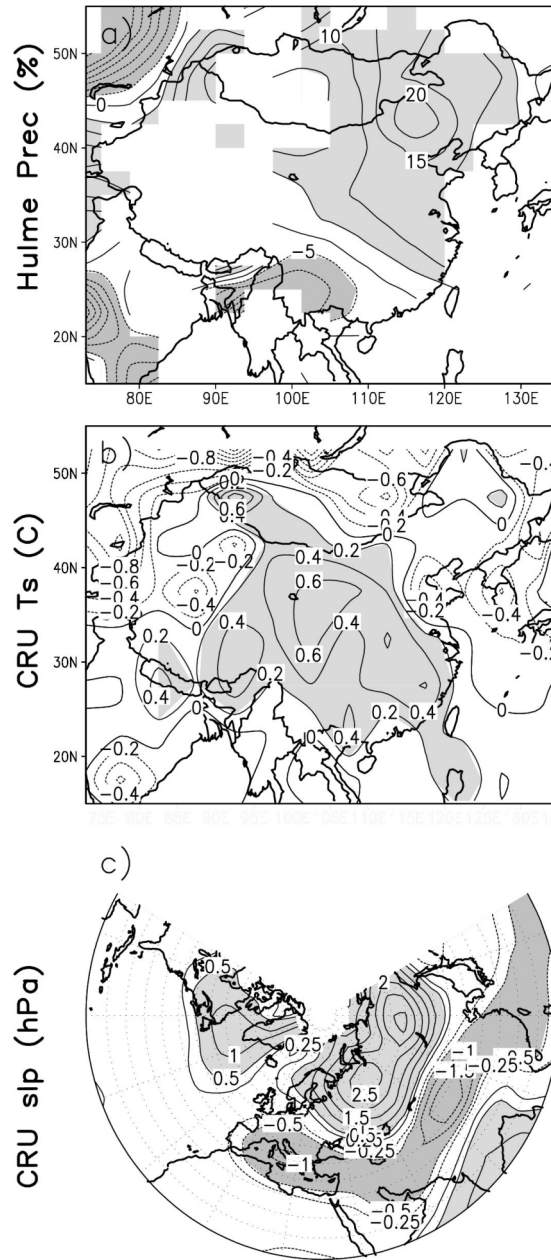


Figure 2. (a) Difference of composite precipitation anomaly percentage (unit: %) for the winters (NDJF) of the AMO warm period (1935/56 - 1955/56) minus the cold period (1970/71-1990/91). (b), as (a), but surface air temperature anomaly (unit: °C). (c), as (a), but sea level pressure (unit: hPa). Shading represents the precipitation anomaly percentage greater (less) than 5% (-5%) in (a), Ts greater than 0.2 in (b), and SLP greater (less) than 0.5 (-0.5) in (c). The contour “0” is omitted in (c). The climatological precipitation used to derive the precipitation anomaly percentage in (a) is the mean through 1951-1980.

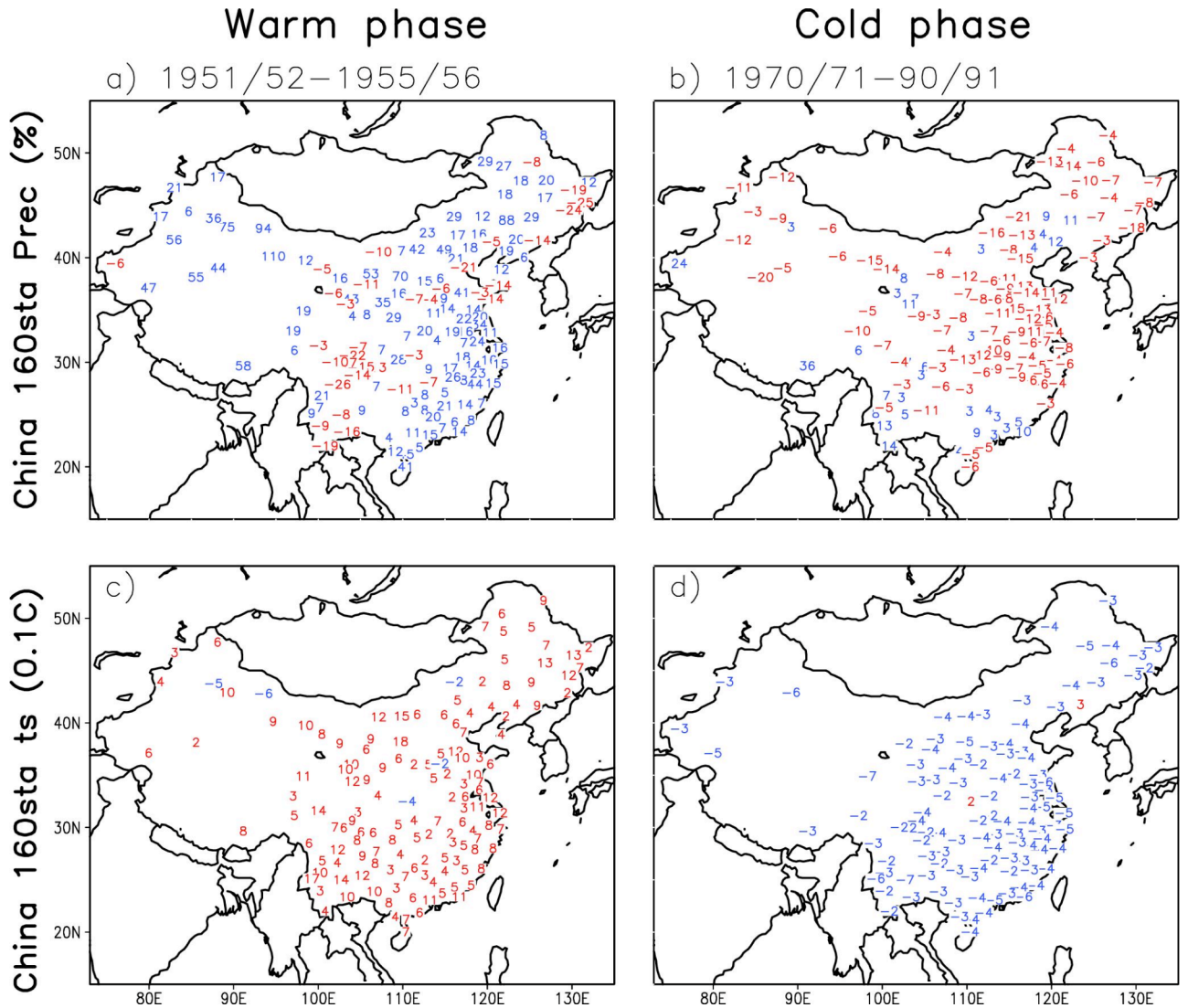


Figure 3. (a) Composite precipitation anomaly percentage when the AMO is warm (1951/52 - 1955/56). (b), as (a), but when the AMO is cold (1970/71-1990/91). (c) (d), as (a) (b), but surface air temperature anomaly. China 160 station dataset is used. Positive (negative) precipitation anomaly percentage values are plotted in blue (red) in (a, b) to indicate being wetter (drier), while sign-reversed Ts values are plotted in these two colors in (c, d) to indicate being colder (warmer). Unit: % in (a, b), and 0.1°C in (c, d).

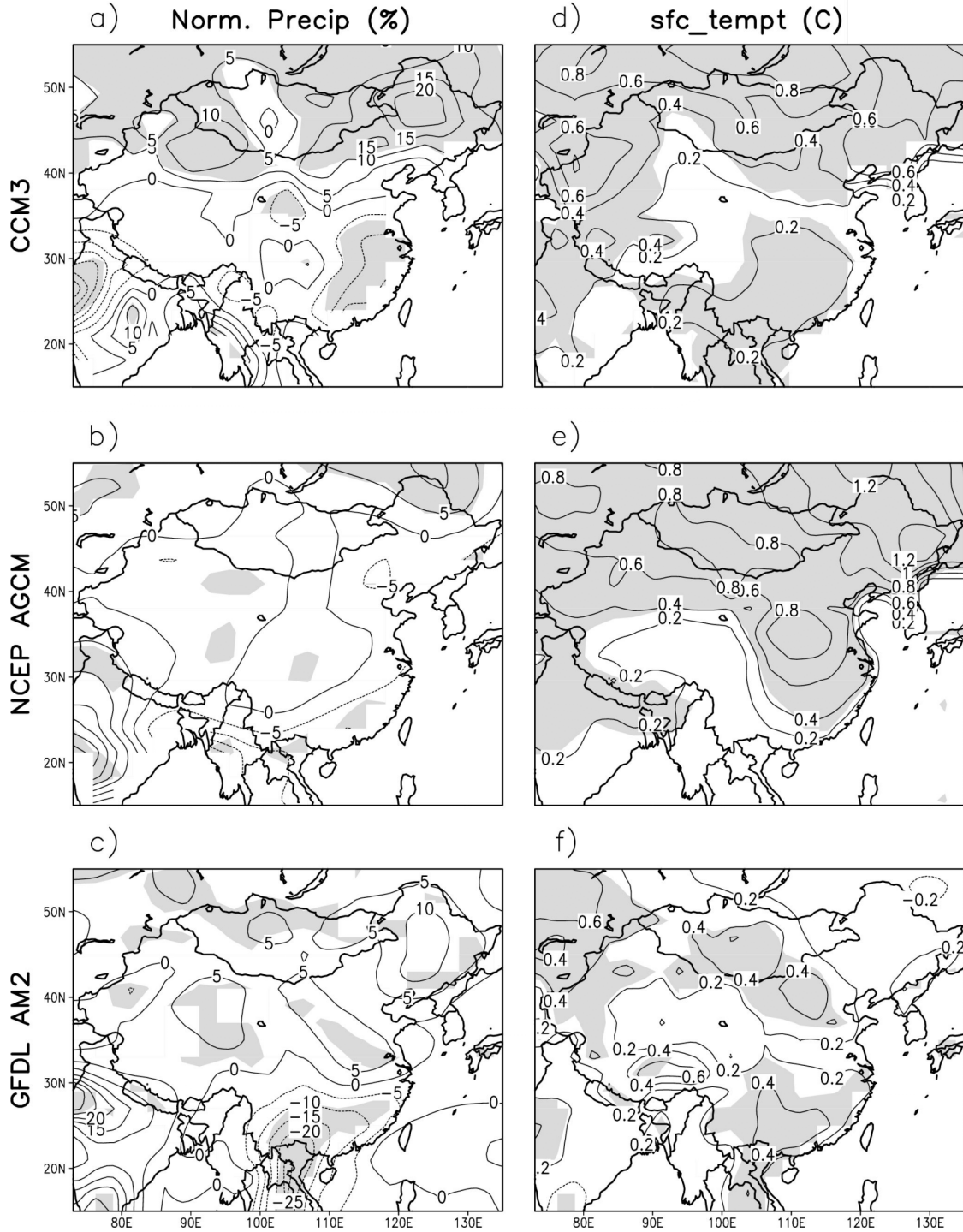


Figure 4. (a) November-February mean response of precipitation anomaly percentage (unit: %) in the NCAR CCM3. (b) (c), as (a), but in the NCEP AGCM and the GFDL AM2, respectively. (d, e, f), as (a, b, c), but for surface air temperature (unit: °C). Shading indicates significant at the level of 95%.

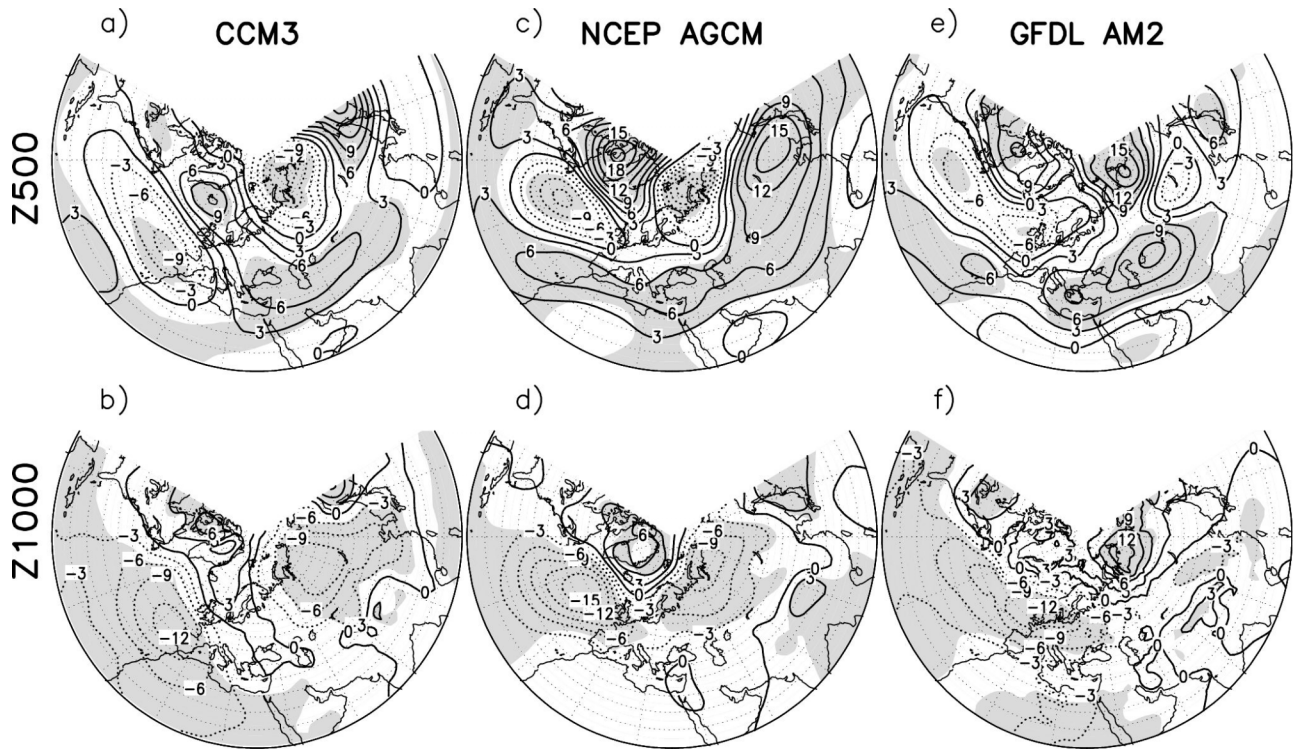


Figure 5. As Fig. 4, but the response of 500-hPa and 1000-hPa geopotential heights. Unit: m.